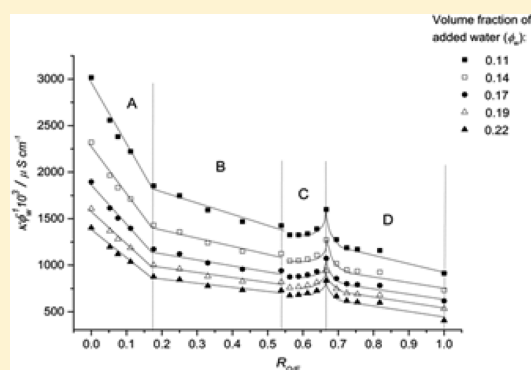


Weak Micelle-Like Aggregation in Ternary Liquid Mixtures as Revealed by Conductivity, Surface Tension, and Light Scattering

Perica Bošković,^{†,‡} Vesna Sokol,[‡] Thomas Zemb,[§] Didier Touraud,[†] and Werner Kunz^{*,†}[†]Institute of Physical and Theoretical Chemistry, University of Regensburg, D-93040 Regensburg, Germany[‡]Department of Physical Chemistry, Faculty of Chemistry and Technology, University of Split, Teslina 10/V, 21000, Split, Croatia[§]Institut de Chimie Séparative de Marcoule, UMR5257 CEA/CNRS/UM2/ENSCM, Bat 426, Marcoule, France

Supporting Information

ABSTRACT: A very small concentration of NaBr is added to ternary, transparent, and thermodynamically stable mixtures of water, ethanol, and octanol. Measuring the electrical conductivity along lines with constant water to ethanol ratios reveals remarkable composition dependencies similar to those found in classical surfactant-based microemulsions. Indeed, light-scattering experiments along the same composition lines and additional surface tension measurements confirm the onset of aggregation and possibly direct, bicontinuous, and reversed structures in these surfactant-free systems such as in classical microemulsions.



1. INTRODUCTION

Microemulsions are transparent, thermodynamically stable, and optically isotropic media consisting of a polar liquid, an apolar one, and at least a surfactant.^{1,2} In the past, thousands of papers have dealt with the four types of microemulsions, as initially identified by Schulmann (Winsor I, II, III, IV),^{3–6} and they have been applied to many fields.^{7–9} In contrast, only a few papers have been concerned with so-called surfactant-free microemulsions (SFME).^{10–20} In recent years, we have been interested in such peculiar systems, because the micellar-like nanostructures form without classical structure-making surfactants.^{17,18,20}

Of course, microheterogeneities often occur not too far from a critical point or a demixing boundary. The groups of Koehler et al. and Schubert et al. studied in detail such micellar and microemulsion structures around the so-called Lifshitz line.^{21,22} However, in these cases, the mixtures contained a hydrotropic ultrashort surfactant. As a result, they found that in certain parts of the phase diagram, even such a hydrotrope can behave as a surfactant. This was detected both for the binary hydrotrope–water and the ternary water–oil–hydrotrope mixtures. Therefore, there is some similarity to our ternary systems as studied here.

However, there is also a significant difference between the systems considered in the present manuscript and those studied by Koehler et al. and Schubert et al.: there is no way to find a surfactant-like behavior in the binary mixtures water/ethanol and octanol/ethanol, which are the corresponding binary systems of our ternary system. Thus, we push the limit of Koehler et al.'s and Schubert et al.'s studies to the case where

not the slightest surfactant-like aggregation behavior of any of the three components is detectable. One may argue that at least octanol is a sort of surfactant. However, in the meantime, we found other systems where typical oils were used, and still the same behavior has been found. The reason why we still consider octanol here is that we have very detailed structural and simulation data on this ternary system and that with the corresponding alkane (octane) the monophasic region is limited to so high ethanol concentrations that even close to the phase boundary microemulsion-like structures no longer occur.

The appearance of microemulsion-like structures in the present water/ethanol/octanol mixtures has been proven without ambiguity by small- (SAXS) and wide-angle X-ray scattering (WAXS), combined with contrast variation small-angle neutron scattering (SANS).²³ The molecule forming the interface between octanol droplets and the water-rich surrounding medium has been found unequivocally as being ethanol: in the systems studied here, the ethanol is the main component of the interfacial film whenever microstructures are present. This situation has been described for the completely surface inactive tannins in ethanol/water solutions.²⁴ The thermodynamic equilibrium between progressive aggregation, universal near a critical point, and aggregation with defined aggregation numbers has been confirmed by molecular dynamics.²⁵

Received: June 29, 2015



One might argue that similar aggregation has already been found previously in even simpler mixtures. A prominent example is the binary mixture of water and acetonitrile,²⁶ and indeed, the SAXS spectra are quite similar to what we found in our ternary system. However, in the case of these completely surfactant-free binary mixtures, there is a significant difference to our system: there is no sign of any preferred size of the detected aggregates, whereas in our mixtures, the probability of finding aggregates with a defined size and interface, just as in the case of classical microemulsions, has become clear, as described in refs 23 and 25. As a result, we believe that the systems that were called SFME on the basis of alkane/water cosolubilization by Keiser et al. and Smith et al.^{10,27} in the 1970s are the missing link between aggregation induced by hydrotropes and surfactants on the one side and systems with random microheterogeneities such as water–acetonitrile mixtures on the other side.

Doubtlessly, SFME clusters are present in many commercial and everyday products, but SFMEs are also used as media for enzymatic reactions,^{14,16} for nanoparticles synthesis,²⁰ for the formulation of insects repellents,¹⁵ and so forth. They permit intimate, yet structured, mixing of oil and water without the disadvantages of the usage of a significant amount of surfactant (ecotoxicity, bad taste, difficult recovery or separation, etc.).

On the basis of microscopy experiments, weak aggregates near a phase separation line in systems containing two slightly miscible solvents and a hydrotropic component could be classified in the following identified topologies: o/w (oil in water) aggregates, w/o (water in oil) aggregates, and bicontinuous nanostructures.²⁸ Interestingly, the existence of these three well-defined microstructures with gradual transformations between them as a function of w/o volume fractions may help us explain paradoxical results obtained during ultracentrifugation, already published in the 1970s.²⁷ Along with suggestions made 40 years ago by Eicke and co-workers, if these transitions occur, slope variations in the equivalent conductivity should appear along dilution lines.^{29–31}

The model system chosen here is the mixture of water, ethanol, and 1-octanol (for simplicity, only octanol in the following). Its phase diagram and all physical chemistry variables in terms of activity and partition coefficients have been determined by Arce et al.⁴² The corresponding phase diagram, as measured again in our lab, is given in Figure 1.

Within the biphasic region, some compositions close to the demixing region show the so-called Ouzo effect, that is, very fine monodisperse emulsions appear spontaneously, and they are surprisingly stable over a certain time, although no surfactant is present to stabilize the droplets.^{32–34}

In the present paper, however, we focus on the transparent, monophasic region of this ternary mixture. We called this part the pre-Ouzo region, emphasizing that there is not yet enough water added to the system (in analogy to the real Ouzo drink) to induce a phase separation and to find the stable Ouzo emulsion. As detailed before, although transparent, the pre-Ouzo mixtures are not homogeneous on a molecular level. In the following, we want to answer the question of how far this microemulsion-like structuring, examined in refs 17, 23, and 25, is also reflected in macroscopic properties such as electric conductivity and surface tension. In fact, such experiments have already been performed for SFMEs in the 1970s,^{27,35} but at that time, it was difficult to distinguish simple molecular fluctuation near a critical point from weak, but defined, aggregation as a consequence of hydration forces balanced by entropy.³⁶

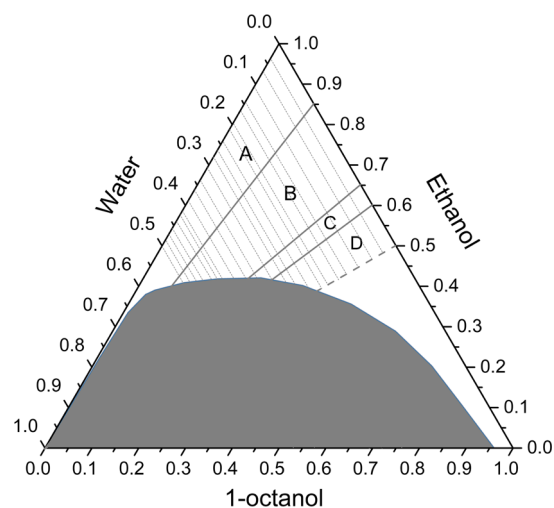


Figure 1. Ternary phase diagram of water/ethanol/octanol mixtures at 298.15 K. The division into areas A–D is deduced from conductivity measurements as shown in Figure 3 and is discussed later. The white region represents compositions of monophasic, clear, macroscopically homogeneous mixtures; the dark region represents compositions of two-phase systems. The values are given in volume fraction.

Dynamic (DLS) combined with static (SLS) light scattering experiments for a broad range of compositions help us to get an idea of the average size of the aggregates: one (DLS) delivers the apparent hydrodynamic size and the other one (SLS) gives the size deduced from the amount of light scattered because of variation of concentrations of the SFMEs. Both are independently determined. Only if the results of both techniques are in agreement, we use them as additional support for the interpretation of the conductivity and surface tension data.

2. EXPERIMENTAL SECTION

2.1. Chemicals. Ethanol (purity $\geq 99.8\%$) and *n*-octanol-1 (purity $\geq 99.0\%$) were purchased from Sigma-Aldrich (Steinheim, Germany). Sodium bromide (suprapure) was purchased from Merck Schuchardt OHG (Hohenbrunn, Germany). All chemicals were used without further purification. All solutions were prepared using deionized water with a resistivity of 18.2 M Ω cm.

2.2. Methods and Techniques. **2.2.1. Ternary Phase Diagram.** For the determination of the phase diagram we followed the procedure described by Clausse et al.³⁷ In test tubes, ethanol was mixed with octanol at determined volume ratios to obtain a starting volume of 25 mL. Water was added dropwise with a micropipette to the resulting mixture until a change in the phase behavior occurred. The added volume amount was recorded. The samples were placed in a water bath at 298.15 K.

2.2.2. Conductometric Measurements. Solutions were prepared as described above. However, in the ternary mixtures, pure water was replaced by a very dilute aqueous salt solution (0.0005 mol/L NaBr), which did not noticeably affect the microstructure or the miscibility gap present in the phase diagram but provided sufficient charge carriers for a detectable signal. In contrast to NaCl, NaBr showed a sufficient solubility in all studied mixtures.

A low-frequency conductivity meter (WTW inoLab Laboratory Conductivity Meters, conductivity cell series Cond

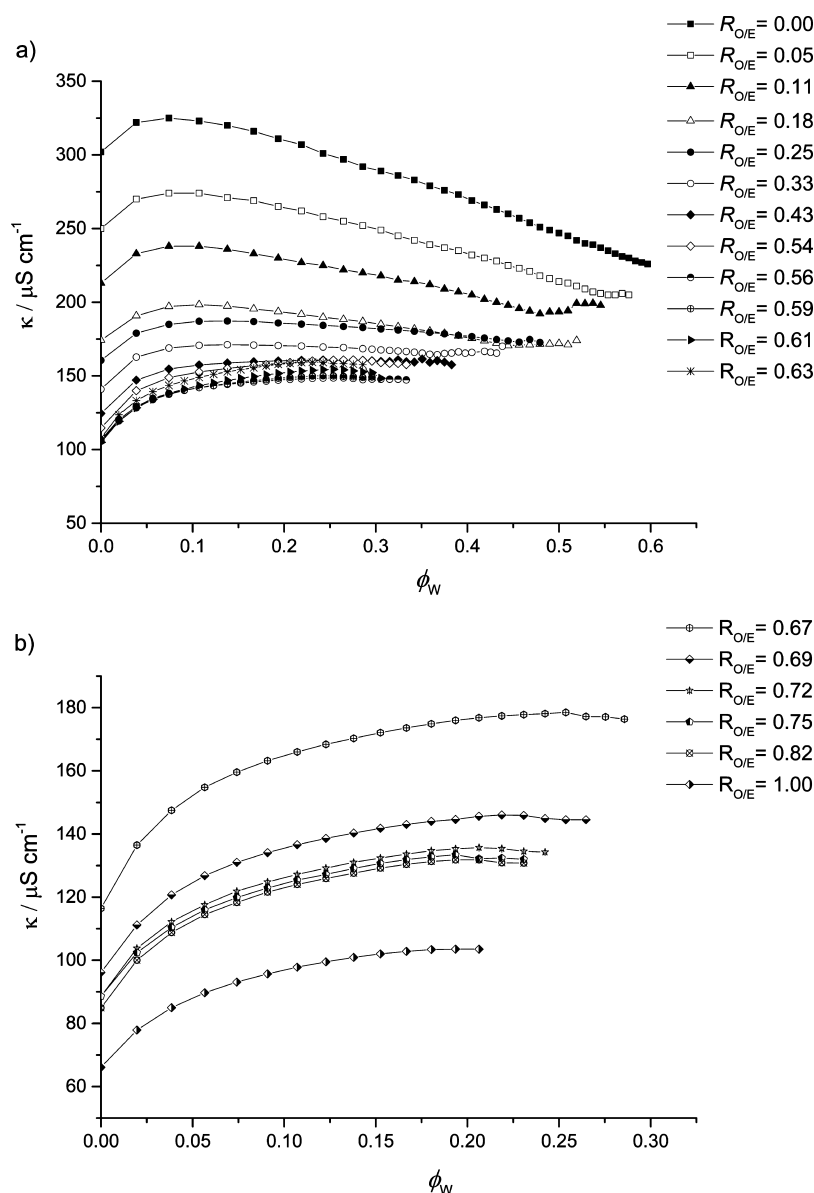


Figure 2. Variation of electrical conductivity κ with water volume fraction (ϕ_w) for the water–octanol–ethanol microemulsion at different volume ratios of octanol to ethanol.

7310) with accuracy of $\pm 1\%$ was used to measure the conductivity of the ternary system with various water volume contents at 298.15 K.

2.2.3. Light Scattering. Dynamic (DLS) and static (SLS) light scattering experiments as well as viscosity measurements have been performed as described in ref 19.

The qualitative agreement of radii inferred from DLS and SLS makes us confident that the approximations (e.g., spherical objects) in our data treatment lead at least semiquantitatively to reliable results. They are also in agreement with simulation and SAXS/SANS scattering results.^{23,25}

2.2.4. Surface Tension. Solutions were prepared as described above. For the surface tension measurements, a solution is transferred into a cylindrical measurement cell and then is inserted into a Force Tensiometer – K100 (Krüss GmbH, Hamburg, Germany) having a measuring range of 1–2000 mN/m and a resolution of 0.001 mN/m. In the present case, the Wilhelmy plate method is used which is based on the force acting on a vertically immersed plate. After equilibration of the

systems, all detections were performed for 300 s at 298.15 \pm 0.1 K.

For the association equilibrium $M_1 \rightleftharpoons (1/g) M_g$ between monomers (M_1) and monodisperse micelles (M_g) with aggregation numbers g , the standard free energy per mole for micelle formation ΔG_m° is given by

$$\Delta G_m^\circ = -RT \ln K = \frac{-RT}{g} \ln x_{M_g} + RT \ln x_{M_1} \quad (1)$$

where R is the universal gas constant, T is the temperature in Kelvin, K is the association constant, and the x symbol represents mole fractions. For large aggregation numbers, the term containing the micellar concentration will vanish and the standard free energy change per monomer may be approximated by

$$\Delta G_m^\circ = RT \ln x_{(M_1)} = RT \ln x_{cmc} \quad (2)$$

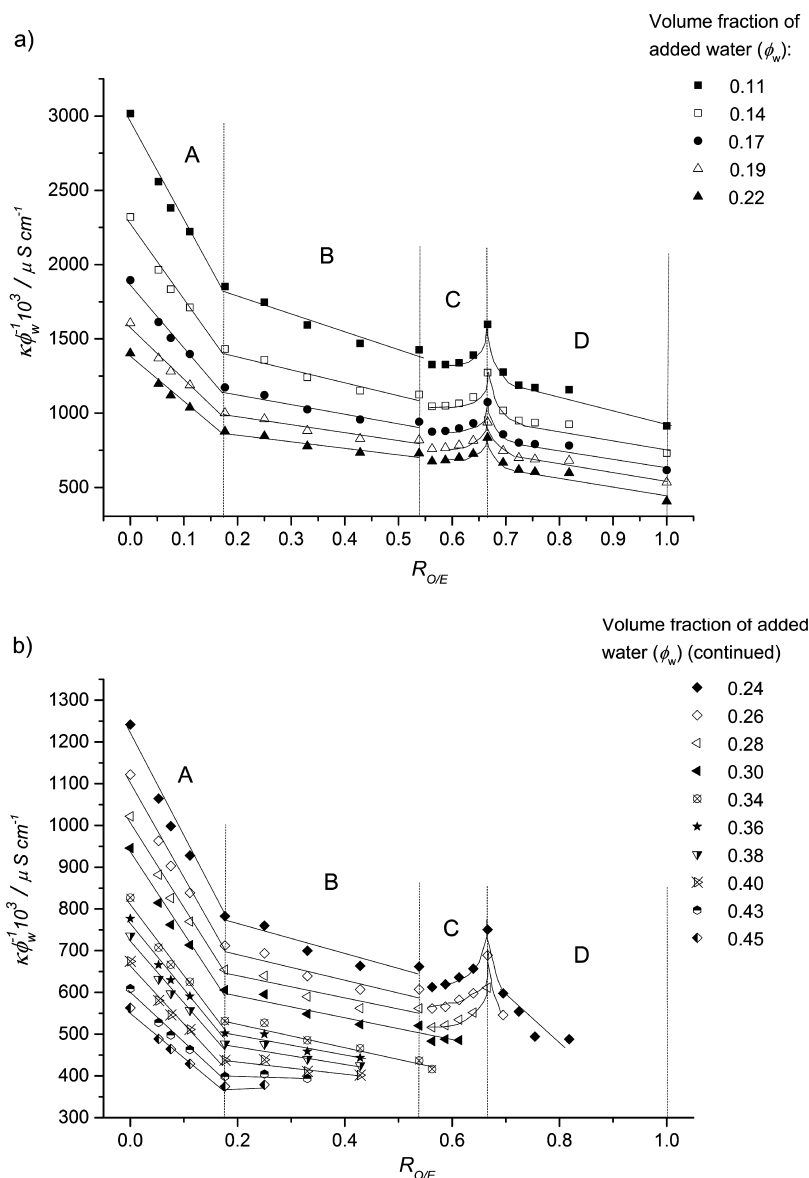


Figure 3. Electrical conductivity (divided by the water volume fraction in analogy to equivalent conductivity in classical binary systems) of the ternary mixtures aqueous solution/ethanol/octanol as a function of different volume ratios of octanol to ethanol ($R_{O/E}$) at constant water volume fraction. The different paths are drawn as dashed lines in Figure 1. A measurable kink in the curves separates areas A–D (see also Figure 1).

3. RESULTS AND DISCUSSION

For solvent-rich microemulsions made with a flexible interface, that is, when the bending constant is low, allowing local curvature variations, the electrical conductivity (κ) changes with increasing water content in the following four successive stages.³⁷ At some stage, the nonlinear increase of κ with an increase of water indicates that the microemulsion system undergoes a gradual structural transition, and around the maximum of the measured conductivity, a bicontinuous microstructure is formed because of the progressive growth and interconnection of the aqueous microdomains. The final decrease of κ with the increase of water content corresponds to the appearance of water-continuous microemulsions. In the case of stiff microemulsions, the behavior is completely different because an antipercolation occurs first, that is, a strong decrease of conductivity occurs when water is added to solvent-rich microemulsions.³⁸ SFME contain only hydrocarbon chains with very flexible short chains, so the weak

aggregation is expected to show gradual transitions from discrete to bicontinuous structures, and inflection points are expected to be seen when specific conductivities are plotted versus increasing amounts of the conducting aqueous solution containing ions as a tracer.

Indeed, this trend was found when plotting the conductivity as a function of brine volume, at least in the intermediate curves of Figure 2a. Figure 2 shows the variations of electrical conductivity κ with water volume fraction (ϕ_w) along dilution lines at different volume ratios of octanol to ethanol. However, we stress that this is a pure macroscopic observation for the moment, and we do not have a detailed microscopic picture of possible bicontinuous or reversed structures. Thus, we cannot exclude that the present observation of the conductivity variation, as shown in Figure 2a and b, has a different molecular origin, when compared to classical microemulsion systems. All the more that even the binary water–ethanol systems exhibits a nonlinear variation of the conductivity.

Keeping in mind that there is no real structuring agent in the mixtures, it is even more surprising to see the strong variation in the conductivity as a function of octanol content at constant water volume ratios, as shown in Figure 3. Four domains (A, B, C, D) are apparent and could correspond to monomers only, pre-Ouzo aggregates, bicontinuous aggregates, and reverse micelles. The conductivity alone does not allow us to draw conclusions on the transformation of microstructures. Also, the onset of micellar-like clustering or a sort of critical micellar or aggregate concentration (cac) has to be confirmed by surface tension and light scattering.³⁹

Therefore, light-scattering experiments have been performed at different compositions of the ternary mixtures. The respective compositions are inserted into the phase diagram and are shown in Figure 4.

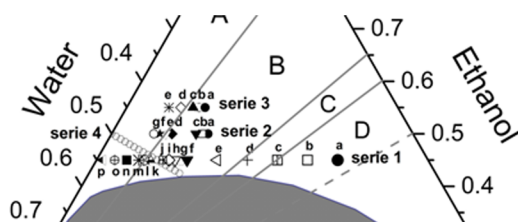


Figure 4. Ternary phase diagram of water/ethanol/octanol mixtures at 298.15 K. Series 1–3 present the compositions of the series of DLS measurements, the results of which are shown in Figures S1–S3 of the Supporting Information. Series 4 presents the compositions of the series of surface tension measurements, the results of which are given in Figure 6. The areas A–D are separated by straight lines.

The different samples are regrouped into four series: series 1–3 contain constant ethanol volume fractions, whereas in series 4, for the surface tension measurements, the water–ethanol volume ratio is kept constant and the octanol content is varied. The DLS correlation functions corresponding to series 1–3 are shown in Figures S1–S3 of the Supporting Information. In the case where these functions are easily distinguished from noise, the radii of the objects are calculated, assuming spherical geometry, as discussed above, in the Experimental Section.

The comparison of radii as derived from DLS and SLS is shown in Figure 5. Especially in the region close to the critical point, where clear autocorrelation functions are detected, there is rough qualitative agreement between the radii deduced from both techniques. The radii as derived from Rayleigh scattering at 45, 90, and 135° do not differ by more than 1%, in contrast to Ornstein–Zernike scattering (scattering due to critical fluctuations), which would give a strong angle dependence. Further, the hydrodynamic radii, as inferred from DLS, are, as expected, higher than the radii derived from the mass of the scattering objects as obtained by SLS, hinting at acceptable approximations in the data processing (object sphericity, etc.).

At lower water content (below 35 vol %) and higher water content (above 48 vol %), no detailed comparison can be drawn for such compositions because of the vanishing autocorrelation functions, as inferred from DLS (see Figure S1 of the Supporting Information). In any case, the origin of the fluctuations seen by light scattering are local fluctuations of aggregates,^{23,25} not fluctuations of individual single molecules, as near critical points of unstructured fluids. Most interestingly, the cluster size drops dramatically (note the logarithmic scale in Figure 5) precisely along the transition line from region B to

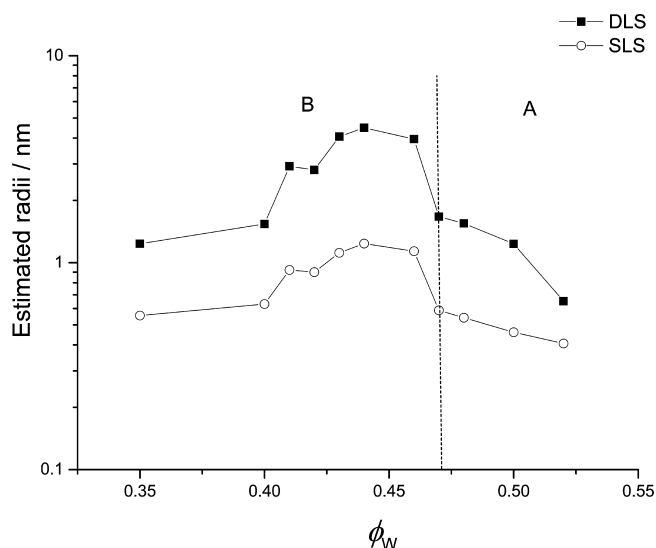


Figure 5. Hydrodynamic radii (DLS) and radii derived from absolute intensity SLS (in nm) versus volume fraction of brine, assuming spherical aggregates. Calculations were carried out for compositions along the path of series 1 (e–p), see Figures 4 and S1 (Supporting Information).

region A. This is proof that the conductivity measurements really reflect the onset of structuring and correspond to a cac in these surfactant-free microemulsions. We do not use the term cmc since this is traditionally used for micelles containing a surfactant.

There is a significant peak in conductivity between the regions C and D. It is reasonable to attribute the appearance of this conductivity maximum to bicontinuous structures in region C continuously changing to reversed micelles in region D, in analogy to typical surfactant systems. However, in contrast to this classical case, where a smooth change in the slope of the conductivity curve is observed, here we have a sharp peak. Such an anomaly is known, for example, from lipid bilayer systems, close to microstructural changes upon adding calcium ions, for instance.⁴⁰

In classical surfactant-based micellar systems, the cmc can also be inferred from the well-known slope change in surface tensions. Figure 6 shows the surface tensions of the ternary mixtures along path 4 in Figure 4. Indeed, a clear change of slope in the surface tension as a function of octanol content is found. As expected, the breakpoint is situated at the border between region A and B in Figure 4, reflecting again a cac , which is approximately 0.5 mol/L (mole fraction $x = 0.03$) of octanol. The corresponding standard free energy change per mole of octanol (see eq 2) is -10 kJ/mol.

Following the classification of Tanford,⁴¹ we consider that around the cac the partition of ethanol within the organic aggregates and outside in the aqueous pseudophase is close to unity.⁴² The pre-Ouzo aggregates formed here are in equilibrium with the bulk pseudophase. The standard free energy of transfer of octanol from the aqueous to the micellar octanol-rich phase is given by the ratio of the mole fractions of octanol in the two pseudophases, and this is $\ln(0.03/0.57) = -2.9 k_B T$ (0.03 is the value at the cac , see above, and 0.57 is deduced from neutron scattering experiments with contrast matching, as will be published separately.).

According to Tanford,⁴³ the corresponding value for a classical aqueous surfactant micellar system would be $-8.3 k_B T$,

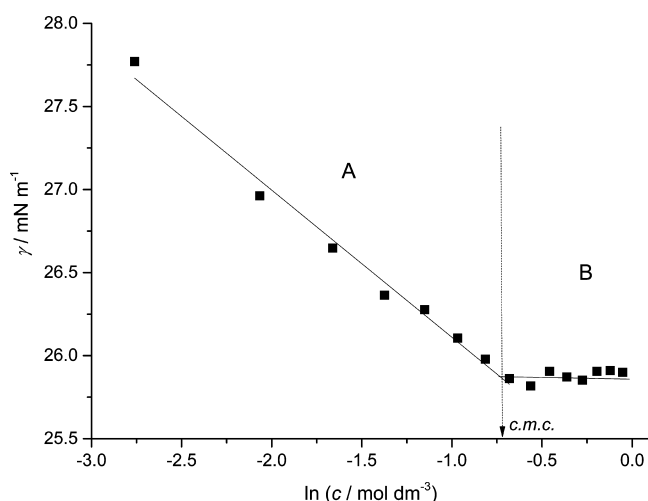


Figure 6. Surface tension values as a function of the logarithm of concentration of octanol at 298.15 K along path 4 drawn in Figure 4.

so in absolute values more than twice as high. This sounds reasonable, since first the aqueous pseudophase contains a significant amount of ethanol, which is of course a much better solvent for octanol compared to pure water, and second, the octanol pseudophase contains also a significant amount of ethanol.

In the present ternary system, the Gibbs absorption isotherm equation cannot be used to determine the excess surface concentration of octanol from the slope of the surface tension curve before the cac, because ethanol is the main component of the interface and usage of the Gibbs law would require the determination of ethanol adsorption excess at constant octanol chemical potential or vice versa. As a consequence, from the present data, the relative contribution of ethanol and octanol cannot be disentangled.

4. CONCLUSIONS

Ternary mixtures of only slightly miscible liquids with a third component that is miscible with both liquids, but not having any aggregation behavior by its own, show significant structuring in the monophasic region close to the miscibility gap, both far and close to the critical point. Inflection points in conductivity (as a function of increasing octanol to ethanol ratios and at constant water content) separate domain A, a simple molecular, unstructured solution, from regions B, C, and D corresponding to the (pseudo)micelle containing o/w pre-Ouzo domain and domains with probably bicontinuous microstructures and reverse micelles, respectively. Two interesting consequences for practical applications may be mentioned: the transition from region A to region B along a change of slope of conductivity exists at high ethanol content, in a domain typically used for perfumes. Moreover, changes of slopes are also found when evaporation rates are plotted versus the amount of oil phase during the transition from o/w to w/o domains, a fact that is widely used in formulation of long-lasting perfume formulation.⁴⁴

■ ASSOCIATED CONTENT

● Supporting Information

Self-correlation functions as inferred from DLS measurements for series 1, as indicated in Figure 4, where the given percentages refer to the volume fraction of water and the

volume fraction of ethanol is 0.45 (Figure S1). Self-correlation functions as inferred from DLS measurements for series 2, as indicated in Figure 4, where the given percentages refer to the volume fraction of water and the volume fraction of ethanol is 0.50 (Figure S2). Self-correlation functions as inferred from DLS measurements for series 3, as indicated in Figure 4, where the given percentages refer to the volume fraction of water and the volume fraction of ethanol is 0.55 (Figure S3). The Supporting Information is available free of charge on the ACS Publications website at DOI: 10.1021/acs.jpcb.5b06228.

■ AUTHOR INFORMATION

Corresponding Author

*E-mail: Werner.Kunz@ur.de.

Notes

The authors declare no competing financial interest.

■ REFERENCES

- (1) Eicke, H. F. Surfactants in Nonpolar Solvents. Aggregation and Micellization. *Top. Curr. Chem.* **1980**, *87*, 85–145.
- (2) Lindman, B.; Wennerstroem, H. *Topics in Current Chemistry (Micelles)*; Springer-Verlag: New York, 1980; pp 1–84.
- (3) Winsor, P. A. Hydrotrophy, Solubilisation and Related Emulsification Processes. *Trans. Faraday Soc.* **1948**, *44*, 376–398.
- (4) Danielsson, I.; Lindman, B. The Definition of Microemulsions. *Colloids Surf.* **1981**, *3*, 391–392.
- (5) Kahlweit, M.; Strey, R.; Haase, D.; Kunieda, H.; Schmeling, T.; Faulhaber, B.; Borkovec, M.; Eicke, H. F.; Busse, G.; Eggers, F.; et al. How to Study Microemulsions. *J. Colloid Interface Sci.* **1987**, *118*, 436–453.
- (6) Kogan, A.; Garti, N. Microemulsions as Transdermal Drug Delivery Vehicles. *Adv. Colloid Interface Sci.* **2006**, *123*, 369–385.
- (7) He, Y.; Li, Z.; Simone, P.; Lodge, T. P. Self-Assembly of Block Copolymer Micelles in an Ionic Liquid. *J. Am. Chem. Soc.* **2006**, *128*, 2745–2750.
- (8) Seth, D.; Chakraborty, A.; Setua, P.; Sarkar, N. Interaction of Ionic Liquids with Water in Ternary Microemulsions (Triton X-100/Water/1-Butyl-3-Methylimidazolium Hexafluorophosphate). *Langmuir* **2006**, *22*, 7768–7775.
- (9) Patrascu, C.; Gauffre, F.; Nallet, F.; Bordes, R.; Oberdisse, J.; de Lauth-Viguerie, N.; Mingotaud, C. Micelles in Ionic Liquids: Aggregation Behavior of alkyl poly(ethyleneglycol)-Ethers in 1-Butyl-3-Methylimidazolium Type Ionic Liquids. *ChemPhysChem* **2006**, *7*, 99–101.
- (10) Keiser, B. A.; Varie, D.; Barden, R. E.; Holt, S. L. Detergentless Water/Oil Microemulsions Composed of Hexane, Water, and 2-Propanol. 2. Nuclear Magnetic Resonance Studies, Effect of Added Sodium Chloride. *J. Phys. Chem.* **1979**, *83*, 1276–1280.
- (11) Lavalley, D. K.; Huggins, E.; Lee, S. Kinetics and Mechanism of the Hydrolysis of Chlorophylla in Ternary Solvent Microemulsion Media. *Inorg. Chem.* **1982**, *21*, 1552–1553.
- (12) Khmelnitsky, Y. L.; van Hoek, A.; Veeger, C.; Visser, A. J. W. G. Detergentless Microemulsions as Media for Enzymatic Reactions: Spectroscopic and Ultracentrifugation Studies. *J. Phys. Chem.* **1989**, *93*, 872–878.
- (13) O'Connor, C. J.; Aggett, A.; Williams, D. R.; Stanley, R. A. Candida Cylindracea Lipase-Catalyzed Hydrolysis of Methyl Palmitate in Detergentless Microemulsion and Paraffin/Water Biphasic Media. *Aust. J. Chem.* **1991**, *44*, 53–60.
- (14) Zoumpantioti, M.; Stamatis, H.; Papadimitriou, V.; Xenakis, A. Spectroscopic and Catalytic Studies of Lipases in Ternary Hexane–1-Propanol–Water Surfactantless Microemulsion Systems. *Colloids Surf., B* **2006**, *47*, 1–9.
- (15) Drapeau, J.; Verdier, M.; Touraud, D.; Kroeckel, U.; Geier, M.; Rose, A.; Kunz, W. Effective Insect Repellent Formulation in both Surfactantless and Classical Microemulsions with a Long-Lasting Protection for Human Beings. *Chem. Biodiversity* **2009**, *6*, 934–947.

- (16) Zoumpantioti, M.; Merianou, E.; Karandreas, T.; Stamatis, H.; Xenakis, A. Esterification of Phenolic Acids Catalyzed by Lipases Immobilized in Organogels. *Biotechnol. Lett.* **2010**, *32*, 1457–1462.
- (17) Klossek, M. L.; Touraud, D.; Zemb, T.; Kunz, W. Structure and Solubility in Surfactant-Free Microemulsions. *ChemPhysChem* **2012**, *13*, 4116–4119.
- (18) Peng, Ni; Wan-Guo, Hou A Novel Surfactant-Free Microemulsion System: *N,N*-Dimethyl Formamide/Furaldehyde/H₂O. *Chin. J. Chem.* **2008**, *26*, 1335–1338.
- (19) Marcus, J.; Klossek, M. L.; Touraud, D.; Kunz, W. Nano-Droplet Formation in Fragrance Tinctures. *Flavour Fragrance J.* **2013**, *28*, 294–299.
- (20) EL-Hefnawy, M. E. Water in Olive Oil Surfactantless Microemulsions as Medium for CdS Nanoparticles Synthesis. *Mod. Appl. Sci.* **2012**, *6*, 101–105.
- (21) Koehler, R. D.; Schubert, K. V.; Strey, R.; Kaler, E. W. The Lifshitz Line in Binary Systems: Structures in Water/C₄E₁ Mixtures. *J. Chem. Phys.* **1994**, *101*, 10843–10849.
- (22) Schubert, K. V.; Strey, R.; Kline, S. R.; Kaler, E. W. Small Angle Neutron Scattering near Lifshitz Lines: Transition from Weakly Structured Mixtures to Microemulsions. *J. Chem. Phys.* **1994**, *101*, 5343–5355.
- (23) Diat, O.; Klossek, M.; Touraud, D.; Deme, B.; Grillo, I.; Kunz, W.; Zemb, T. Octanol-Rich and Water-Rich Domains in Dynamic Equilibrium in the Pre-Ouzo Region of Ternary Systems Containing a Hydrotrope. *J. Appl. Crystallogr.* **2013**, *46*, 1665–1669.
- (24) Zanchi, D.; Vernhet, A.; Poncet-Legrand, C.; Cartalade, D.; Tribet, C.; Schweins, R.; Cabane, B. Colloidal Dispersions of Tannins in Water–Ethanol Solutions. *Langmuir* **2007**, *23*, 9949–9959.
- (25) Schöttl, S.; Marcus, J.; Diat, O.; Touraud, D.; Kunz, W.; Zemb, T.; Horinek, D. Emergence of Surfactant-Free Micelles From Ternary Solutions. *Chem. Sci.* **2014**, *5*, 2949–2954.
- (26) Takamuku, T.; Noguchi, Y.; Matsugami, M.; Iwase, H.; Otomo, T.; Nagao, M. Heterogeneity of Acetonitrile–Water Mixtures in the Temperature Range 279–307 K Studied by Small-Angle Neutron Scattering Technique. *J. Mol. Liq.* **2007**, *136*, 147–155.
- (27) Smith, G. D.; Donelan, C. E.; Barden, R. E. Oil-Continuous Microemulsions Composed of Hexane, Water, and 2-Propanol. *J. Colloid Interface Sci.* **1977**, *60*, 488–496.
- (28) Xu, Jie; Yin, Aolin; Zhao, Jikuan; Li, Dongxiang; Hou, W. G. Surfactant-Free Microemulsion Composed of Oleic Acid, n-Propanol, and H₂O. *J. Phys. Chem. B* **2013**, *117*, 450–456.
- (29) Eicke, H. F.; Christen, H. Is Water Critical to the Formation of Micelles in Apolar Media? *Helv. Chim. Acta* **1978**, *61*, 2258–2263.
- (30) Eicke, H. F. *Topics in Current Chemistry (Micelles)*; Springer-Verlag: New York, 1980; pp 85–145.
- (31) Eicke, H. F.; Borkovec, M.; Das-Gupta, B. Conductivity of Water-in-Oil Microemulsions: a Quantitative Charge Fluctuation Model. *J. Phys. Chem.* **1989**, *93*, 314–317.
- (32) Preu, H.; Schirmer, C.; Tomšić, M.; Bešter Rogač, M.; Jamnik, A.; Belloni, L.; Kunz, W. Light, Neutron, X-ray Scattering, and Conductivity Measurements on Aqueous Dodecyltrimethylammonium Bromide/1-Hexanol Solutions. *J. Phys. Chem. B* **2003**, *107*, 13862–13870.
- (33) Peng, S.; Xu, C.; Hughes, T. C.; Zhang, X. From Nanodroplets by the Ouzo Effect to Interfacial Nanolenses. *Langmuir* **2014**, *30*, 12270–12277.
- (34) Zhang, X. H.; Ducker, W. Interfacial Oil Droplets. *Langmuir* **2008**, *24*, 110–115.
- (35) Pulg, J. E.; Hemker, D. L.; Gupta, A.; Davis, H. T.; Scriven, L. E. Interfacial Tensions and Phase Behavior of Alcohol-Hydrocarbon-Water-Sodium Chloride Systems. *J. Phys. Chem.* **1987**, *91*, 1137–1143.
- (36) Parsegian, V. A.; Zemb, T. Hydration Forces: Observations, Explanations, Expectations, Questions. *Curr. Opin. Colloid Interface Sci.* **2011**, *16*, 618–624.
- (37) Clausse, M.; Nicolas-Morgantini, L.; Zradba, A.; Tourand, D. *Microemulsion Systems*; M. Dekker: New York, 1987; pp 387–401.
- (38) Zemb, T. N. The DOC Model of Microemulsions: Microstructure, Scattering, Conductivity and Phase Limits Imposed by Sterical Constraints. *Colloids Surf., A* **2003**, *129*, 435–454.
- (39) Chevalier, Y.; Zemb, T. The Structure of Micelles and Microemulsions. *Rep. Prog. Phys.* **1990**, *53*, 279–371.
- (40) Uhríková, D.; Kučerka, N.; Teixeira, J.; Gordeliy, V.; Balgavý, P. Structural Changes in Dipalmitoylphosphatidylcholine Bilayer Promoted by Ca²⁺ Ions: a Small-Angle Neutron Scattering Study. *Chem. Phys. Lipids* **2008**, *155*, 80–89.
- (41) Tanford, C. *The Hydrophobic Effect: Formation of Micelles and Biological Membranes*; Wiley: New York, 1980.
- (42) Arce, A.; Blanco, A.; Soto, A.; Vidal, I. Densities, Refractive Indices, and Excess Molar Volumes of the Ternary Systems Water + Methanol + 1-Octanol and Water + Ethanol + 1-Octanol and Their Binary Mixtures at 298.15 K. *J. Chem. Eng. Data* **1993**, *38*, 336–340.
- (43) Tanford, C. Theory of Micelle Formation in Aqueous Solutions. *J. Phys. Chem.* **1974**, *78*, 2469–2479.
- (44) Tchakalova, V.; Zemb, T.; Benczedi, D. Evaporation Triggered Self-Assembly in Aqueous Fragrance-Ethanol Mixtures and Its Impact on Fragrance Performance. *Colloids Surf., A* **2014**, *460*, 414–421.